

scientific data



OPEN

DATA DESCRIPTOR

The 626M24 dataset of validated transitions and empirical rovibrational energy levels of $^{16}\text{O}^{12}\text{C}^{16}\text{O}$

Ala'a A. A. Azzam¹✉, Dunia Alatoom^{1,2,3}, Bashar M. J. Abou Doud¹, Meera Q. A. Shersheen^{1,2}, Bailasan K. M. Almasri¹, Celin N. M. Bader^{1,2,4}, Baraa O. A. Kh. Musleh^{1,2,5}, Maria Zakaria Jado Obaido^{1,2,6}, Ahmad M. H. Abu Khudair^{1,2,7}, Adam W. M. Al Shatarat^{1,2,5}, Bana I. M. Qattan^{1,2,8}, Loay H. M. Hamamsy^{1,2,9}, Abdullah O. G. Saafneh^{1,2,10}, Mohammad N. A. ALSo'ub^{1,2,11}, Mera M. A. Alkhashashneh^{1,2,12}, Haneen O. M. Al-Zawahra^{1,2,13}, Mohammad Taha I. Ibrahim^{1,2,3}, Jonathan Tennyson^{1,3}✉, Sergei N. Yurchenko¹, Tibor Furtenbacher^{1,4} & Attila G. Császár^{1,4}✉

The 626M24 dataset created during this project contains validated experimental transitions and empirical rovibrational energy levels for the parent carbon dioxide isotopologue, $^{12}\text{C}^{16}\text{O}_2$ (in a shorthand notation, 626). Validation of the measured transitions and determination of the empirical energy levels is based on a compiled and carefully checked dataset of experimental rovibrational transitions collected from 143 literature sources. The 44 828 measured lines collected, in the wavenumber range of 42.9 – 14 076 cm⁻¹, describe 22 218 unique transitions. Inversion of the experimental information yields 8268 empirical rovibrational energy levels for 626, with uncertainty estimates compliant with the experimental uncertainties of the transitions. Comparison with the Carbon Dioxide Spectroscopic Databank (CDSD-296), NASA Ames-2021, and HITRAN2020 line catalogues shows generally good agreement and suggests some possible improvements to these databases. The 626M24 dataset and an extended line list, called 626M24LL, built upon it and containing 285 503 line positions, are deposited in an OSF (Open Science Framework) repository.

Background & Summary

The triatomic carbon dioxide molecule, CO₂, contains two terminal oxygen and a single central carbon atom, and in the electronic ground state it has a linear equilibrium structure. Studying the internal motions and related rovibrational spectra of carbon dioxide at relatively low temperatures, so that none of the excited electronic states need to be taken into account, is relevant to many fields of science and technology.

The variation in the CO₂ content of the atmosphere of Earth over time is one of its important characteristics¹. Detailed understanding of CO₂ spectroscopic features^{2,3}, in particular the line center positions, both with and without collisional effects, helps to establish the total amount and the distribution of this molecule in the

¹Department of Physics, The University of Jordan, Queen Rania St, Amman, Jordan. ²Research Department, AstroJo Institute, Wasfi Al-Tal St, Amman, Jordan. ³Department of Physics and Astronomy, University College London, Gower Street, London, WC1E 6BT, UK. ⁴Pioneer Educational Schools, Dhi Al Qaada, Amman, Jordan. ⁵Bunat AlGhad Academy, Shaher Abu Haya, Aws Ben Thabet St., Amman, Jordan. ⁶First University Schools, Jubaihah, Ahmad Altarawneh St., Amman, Jordan. ⁷International Grand Academy, GW3J+6VQ, Petra St., Aydoun, Jordan. ⁸Islamic Educational College, 2V8R+GV6, Al-Hakem An-Nisabouri St., Amman, Jordan. ⁹Modern Systems Schools, Tla'a Al Ali, Amman, Jordan. ¹⁰AlJami'a AlOula Schools, Ahmad Al-Tarawneh 65, Amman, Jordan. ¹¹Mada International Academy, King Abdullah II St. 379, Amman, Jordan. ¹²The Jubilee School, 2WJ2+VFH, Muhammad An-Nejdawi St., Amman, Jordan. ¹³AlHassad AlTarbawi Schools, VVPW+X6M, At-Tahrir St., Amman, Jordan. ¹⁴ELTE Eötvös Loránd University, Institute of Chemistry, H-1117, Budapest, Pázmány Péter sétány 1/A, Hungary. ✉e-mail: alaa.azzam@ju.edu.jo; j.tennyson@ucl.ac.uk; attila.csaszar@ttk.elte.hu

Isotopologue	No. of levels	$\Delta E_{\text{Ames}-2021}^{\text{MAD}}$	$\Delta E_{\text{Ames}-2021}^{\text{AAD}}$	$\Delta E_{\text{CDSD}-296}^{\text{MAD}}$	$\Delta E_{\text{CDSD}-296}^{\text{AAD}}$
$^{16}\text{O}^{12}\text{C}^{16}\text{O}$ (626) [This work]	8268	0.147	0.015	0.077	0.001
$^{16}\text{O}^{12}\text{C}^{18}\text{O}$ (628) ²⁵	8786	0.231	0.022	0.182	0.002
$^{16}\text{O}^{13}\text{C}^{16}\text{O}$ (636) ²⁶	6318	0.152	0.016	0.081	0.002
$^{16}\text{O}^{13}\text{C}^{18}\text{O}$ (638) ²⁷	3975	0.151	0.024	0.268	0.002
$^{18}\text{O}^{12}\text{C}^{18}\text{O}$ (828) ²⁸	3923	0.571	0.042	0.559	0.002
$^{17}\text{O}^{12}\text{C}^{18}\text{O}$ (728) ²⁸	4318	0.109	0.024	0.046	0.001
$^{18}\text{O}^{13}\text{C}^{18}\text{O}$ (838) ²⁸	1058	0.168	0.045	0.039	0.001

Table 1. The number of empirical (MARVEL) rovibrational energy levels determined, and the maximum absolute (MAD) and average absolute (AAD) energy level differences, ΔE , in hc cm^{-1} , between the MARVEL studies and those from Ames-2021²² and CDSD-296²¹ for isotopologues of carbon dioxide studied by our group^{25–28}.

atmosphere of Earth. These data also help to understand the effect of CO_2 on a number of environmental issues, such as climate change and the radiative balance of our atmosphere. The industrial revolution has had a significant impact on climate change; during the last century, the well-documented increase of CO_2 's concentration in the atmosphere of the Earth is predominantly due to human activity⁴. Approximately 98.45 % of carbon dioxide molecules in the atmosphere of the Earth are in the form of the parent, $^{16}\text{O}^{12}\text{C}^{16}\text{O}$ isotopologue, making it the most important isotopologue to study.

Carbon dioxide plays a crucial role in many areas of astronomical research as well, from the study of stars^{5,6} to the exploration of planetary atmospheres^{7–9}; in our own solar system, carbon dioxide is the major constituent and thus determines the radiative balance of the atmospheres of the planets Mars and Venus. The detection and characterization of CO_2 absorption features in exoplanetary spectra offer clues about the atmospheric composition, pressure, and temperature profiles of these distant worlds. CO_2 was one of the first molecules detected in the atmosphere of an exoplanet¹⁰ and several recent observations have been made using the James Webb Space Telescope¹¹. Within the dense molecular clouds that pervade the interstellar medium, CO_2 serves as an important tracer of the physical and chemical conditions that govern the birth of new stars^{12,13}. Emissions from the bending states of the CO_2 isotopologues in the far infrared provide valuable information on the temperature, density, and kinematics of these star-forming regions¹².

Remote sensing of the CO_2 content of the Earth's atmosphere is a major activity aimed at monitoring the carbon content of our atmosphere in increasing detail. Missions such as NASA's OCO-2 and OCO-3 satellites and ESA's planned CO2M satellite constellation have stringent requirements on laboratory spectroscopy results, required for the interpretation of their observations^{14,15}. Similar accuracy is required for ground-based spectroscopic experiments such as TCCON (Total Carbon Column Observing Network)¹⁶.

CO_2 spectra are important for medical¹⁷ and industrial applications¹⁸, as well. The study of CO_2 spectra in plasma physics is widespread¹⁹, where there is particular emphasis on the use of plasma processes to valorize excess CO_2 from the Earth's atmosphere²⁰.

Due to the importance of accurate high-resolution spectroscopic data related to carbon dioxide, they are available in several line-by-line spectroscopic databases, such as the Carbon Dioxide Spectroscopic Databank (CDSD-296)²¹, NASA Ames-2021²², HITRAN2020²³, and ExoMol²⁴. The present report on the spectroscopic data of $^{16}\text{O}^{12}\text{C}^{16}\text{O}$ (626) is part of a long-term, ongoing project devoted to the construction of the most extensive empirical energy level datasets, calculated from measured line positions in high-resolution rovibrational spectra, for all isotopologues of carbon dioxide involving the ^{12}C , ^{13}C , ^{16}O , ^{17}O , and ^{18}O isotopes. Empirical energy levels based on *all* the measured rovibrational transitions are already available for the carbon dioxide isotopologues $^{16}\text{O}^{12}\text{C}^{18}\text{O}$ (628)²⁵, $^{16}\text{O}^{13}\text{C}^{16}\text{O}$ (636)²⁶, $^{16}\text{O}^{13}\text{C}^{18}\text{O}$ (638)²⁷, $^{18}\text{O}^{12}\text{C}^{18}\text{O}$ (828)²⁸, $^{17}\text{O}^{12}\text{C}^{18}\text{O}$ (728)²⁸, and $^{18}\text{O}^{13}\text{C}^{18}\text{O}$ (838)²⁸ (see Table 1). In these projects, empirical energy levels are calculated using the MARVEL 4.0 (Measured Active Rotational-Vibrational Energy Levels) procedure^{29–32}, built upon the theory of spectroscopic networks^{33,34}. Statistical measures of these previous studies, mostly with respect to the Ames-2021²² and CDSD-296²¹ datasets of energy levels are also given in Table 1. For the seven isotopologues studied thus far, agreement with the CDSD-296 data is significantly better, by more than an order of magnitude for the average absolute deviation.

The most important results of this study, obtained with the help of the MARVEL code for the 626 isotopologue of carbon dioxide, include the 626M24 dataset of validated experimental transitions and empirical rovibrational energy levels, and a large rovibrational line list, 626M24LL. All of these data will contribute not only to future spectroscopic measurements on carbon dioxide but also to the refinement of theoretical and computational spectroscopic models and the enhancement of spectroscopic line-by-line databases, such as HITRAN²³ and ExoMol^{24,35}.

Methods

Source data. References^{36–180} contain rovibrational transitions data considered during the MARVEL analysis of this study. The wavenumber range covered by these measurements is limited to $42.9 - 14\,076 \text{ cm}^{-1}$.

MARVEL. The MARVEL procedure^{29–32}, used extensively during this study, starts with the careful collection, detailed examination, and subsequent validation of the positions of transitions in high-resolution (laboratory) spectra. The transitions collected are then used to construct a spectroscopic network (SN)^{33,34}, whereby each

energy level serves as a node and the nodes are interconnected by the observed transitions. The SN built allows the determination of empirical energy-level values along with educated estimates for their uncertainties³². Unlike the effective Hamiltonians widely used for spectroscopic analysis, the MARVEL approach is model-free. This has a number of advantages and, in particular, for the CO₂ molecule with its many resonances, MARVEL does not require any special measures or extra parameters to characterize levels perturbed by “accidental” interactions with nearby states.

Ideally, the experimentally observed transitions allow the creation of a well-connected SN, linking all transitions to the ground state (defined as the state with no rovibrational excitation), called the root of the SN. However, because of the limited coverage offered by the experimental data, this is usually not the case. Therefore, in practice, the SN can become fragmented, resulting in a principal component, where all the nodes are linked to the root, and a number of isolated, so-called floating components with their own roots.

The MARVEL protocol allows for the detection of inconsistencies, that is, lines that are in conflict with the correct measurement data. This feature proves invaluable for identifying issues with experimental data that usually come from several sources, such as user errors made during data collection and analysis, incorrect assignments, or the use of different naming conventions.

Notation and quantum numbers. CO₂ has three fundamental vibrational modes, conventionally denoted as ν_1 , ν_2 , and ν_3 , associated with the vibrational quantum numbers v_i , $i = 1, 2$, and 3 , respectively. The two-dimensional (degenerate) bending mode, ν_2 , is characterized by an angular momentum, described by the quantum number ℓ_2 . Herzberg’s notation is often used to assign energy levels in triatomics; in this notation, the vibrational states of CO₂ are designated as $(\nu_1 \nu_2^{\ell_2} \nu_3)$. For the CO₂ molecule with a linear equilibrium structure in its ground electronic state, there is a strong Fermi-resonance interaction between the states $(\nu_1 (\nu_2 + 2)^{\ell_2} \nu_3)$ and $(\nu_1 + 1 \nu_2^{\ell_2} \nu_3)$. Therefore, it became customary to employ the so-called AFGL (Air Force Geophysics Laboratory) notation to denote the vibrational states and bands of CO₂ isotopologues. In the AFGL notation^{181–183}, the vibrational energy levels are designated by the quintuplet $(\nu_1 \nu_2 \ell_2 \nu_3 r)$, where r is the ranking index for states in Fermi resonance (the r index is used to distinguish the levels belonging to the same Fermi polyad). The lowest value of r , 1 , is assigned to the energy level with the highest wavenumber (or frequency), and r increases for lower-energy levels. For example, the three vibrational states $(2\ 0\ 0\ 0)$, $(1\ 2\ 0\ 0)$, and $(0\ 4\ 0\ 0)$ are in Fermi resonance with each other and have the AFGL vibrational descriptors $(2\ 0\ 0\ 0\ 3)$, $(2\ 0\ 0\ 0\ 2)$, and $(2\ 0\ 0\ 0\ 1)$, respectively.

It is customary to use polyad numbers P to denote strongly interacting groups of vibrational states, decoupling them from the other vibrations. This is a useful concept, especially when effective Hamiltonians are formed. P is not a quantum number, but it behaves like one. For carbon dioxide, based on the approximate relations of the harmonic frequencies, $\omega_1 \approx 2\omega_2$ and $\omega_3 \approx 3\omega_2$, the widely accepted definition of P , also used in this study, is $P = 2\nu_1 + \nu_2 + 3\nu_3$.

The quantum number J is used to denote the angular momentum associated with rotational and (when $\ell_2 > 0$) vibrational motion of the CO₂ molecule. Transitions with $\Delta J = -1$ and $\Delta J = +1$ are called the P- and R-branch transitions, respectively, while the Q-branch transitions are associated with $\Delta J = 0$. P and R transitions occur in both the parallel and perpendicular bands, while the Q branch transitions only occur in the parallel bands, where the direction refers to the change in the dipole moment driving the transition relative to the linear equilibrium structure of the molecule. For the symmetric isotopologue 626, the Pauli principle means that symmetric vibrational states (those with even ν_3 values) only have even J levels, while anti-symmetric vibrational states (those with odd ν_3 values) have only odd J levels. Similarly, for states with even values of $J + \ell_2 + \nu_3$ the rotationless parity is ‘e’, while for states with odd $J + \ell_2 + \nu_3$ values the rotationless parity is ‘f’. The coupling of rotational and vibrational angular momentum means that $J \geq \ell_2$.

The upper and lower states involved in a transition are denoted as ‘’ and ‘”, respectively, and the P, R, and Q transitions are usually specified using the lower-state rotational quantum number (J''). For the purposes of the MARVEL analysis, each state is uniquely characterized using the set of seven descriptors $(J \nu_1 \nu_2 \ell_2 \nu_3 r e/f)$. This is the format followed by the data deposited in the Supplementary Material to this paper.

Data Records

The 626M24 dataset is available in an OSF (Open Science Framework) repository¹⁸⁴. It contains (a) all experimentally measured transitions collected during this work, (b) all empirical rovibrational energy levels determined, and (c) an extensive line list derived from the levels. All validated transitions have positive wavenumber or frequency values, while transitions that had to be removed have negative values. The same repository contains a table describing the main characteristics of the 143 literature sources that contain the transitions collected and analyzed.

The file “626M24_segments.txt” is the segment input file utilized by the MARVEL code, where the unit of the line positions and their uncertainties are specified for each data source. The file “626M24_transitions.txt” contains the 44 828 input transitions, collected from Refs. ^{36–180}, used during the MARVEL analysis. In this file, each transition is characterized by (a) a line position (in units stored in the segment file), (b) an initial and an adjusted line-position uncertainty, (c) the rovibrational assignments for the upper and lower states (see the previous section for a description), and (d) a line tag, representing a unique identifier (each data source tag is based on the last two digits of the year of publication and the first two characters of the last names of the authors).

Of all the experimentally measured transitions only about half of them, 22 218, are unique. During the MARVEL analysis, 368 transitions had to be removed from our spectroscopic network; note, in particular, that all the measured transitions of 00TaPeTeLe¹⁰⁷ had to be deleted. It is also worth mentioning that although the transitions of the sources 94Bailly⁹³ and 97BaCaLa⁹⁷ are included in the transition file, the transitions reported in them form floating components. Thus, we cannot independently validate them or determine the absolute values of the energy levels associated with them. Finally, it is important to add that although most of the transitions in

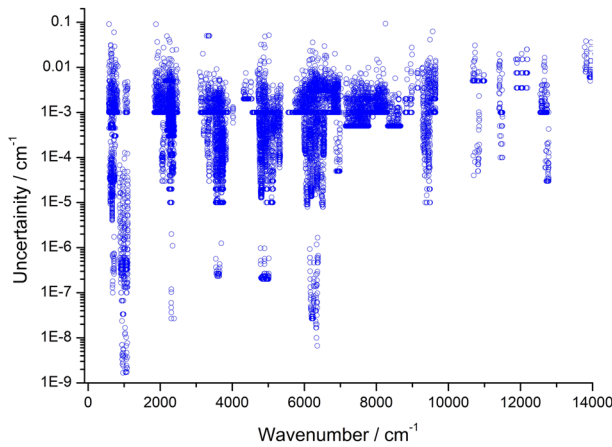


Fig. 1 Uncertainties of the experimental rovibrational line-center positions available for the $^{16}\text{O}^{12}\text{C}^{16}\text{O}$ molecule, as a function of the transition wavenumber (note the logarithmic scale of the vertical axis). If multiple measurements are available for the same line, the most accurate transition is chosen.

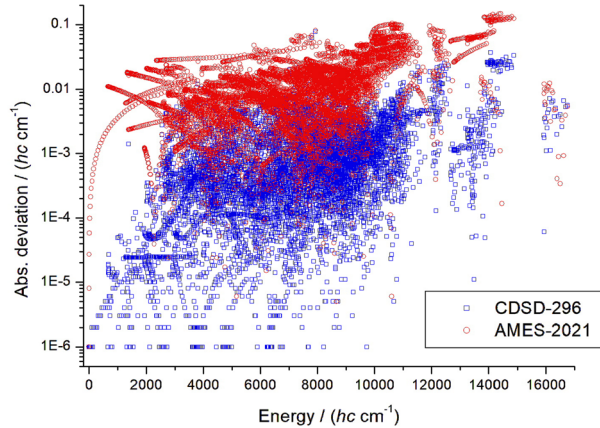


Fig. 2 Comparison between rovibrational energies of the present $^{16}\text{O}^{12}\text{C}^{16}\text{O}$ dataset and those of CDSD-296²¹ (blue squares) and Ames-2021²² (red circles).

the transition file “626M24_transitions.txt” are from measurements, the final dataset also contains calculated line positions. These sources are denoted by ‘_C’ in the tag. The reason to include these calculated line positions in the transitions list is that the uncertainty of these lines is several orders of magnitude smaller than that of other transitions measured in the given region and they help the analysis of the spectroscopic network of 626.

The empirical energy values, obtained for 8268 rovibrational states in the $0 - 20654\text{ cm}^{-1}$ range, are placed in the file “626M24_energy_levels.txt”. Each energy level of this data file is characterized by (a) a rovibrational label, (b) an empirical (MARVEL) energy in hc cm^{-1} , (c) an energy uncertainty in hc cm^{-1} , and (d) the number of transitions incident to this state.

Using our empirical energies and the CDSD-296²¹, NASA Ames-2021²², and HITRAN2020²³ line positions and intensities, an extended line list, named 626M24LL, was constructed, given in the file “626M24_line_list.txt”. Line intensities relate the probability of absorption by a given line at a specified temperature; here we adopt the standard HITRAN²³ unit of cm molecule^{-1} . This line list contains 285 503 dipole-allowed transitions in the range $147 - 19909\text{ cm}^{-1}$, with room-temperature intensities down to $10^{-31}\text{ cm molecule}^{-1}$. Columns (1) – (21) of the “626M24_line_list.txt” file contain the following information: (1) CDSD-296 line position, (2) AMES-21 line position, (3) HITRAN2020 line position, (4) MARVEL line position (generated from the MARVEL energy levels as $E_{\text{up},\text{MARVEL}} - E_{\text{low},\text{MARVEL}}$), (5) MARVEL uncertainty, (6) AMES-21 intensity (100% abundance assumed), (7) HITRAN2020 line intensity (scaled by natural abundance), (8–14) descriptors of the upper state, and (15–21) descriptors of the lower state. All line positions and uncertainties are in cm^{-1} , the intensity values correspond to a temperature of 296 K. Beyond column (21) the line may contain a possible comment. Four types of comments are used: (a) ‘ONLY IN MARVEL’ means that this line can only be found in the experimental transitions dataset, but not in CDSD-296 and HITRAN2020. There are 290 such lines in the 626M24 dataset, typically with high v_3 values ($v_3 > 6$). (b) The 626M24 dataset contains 2506 lines that can be found ‘ONLY IN HITRAN’. Most of these lines (2134) are not assigned (their vibrational labels are $-2 - 2 - 2 0$). (c) When the deviation of the HITRAN2020 position from the CDSD-296 and/or MARVEL positions is larger than 0.01 cm^{-1} , the comment

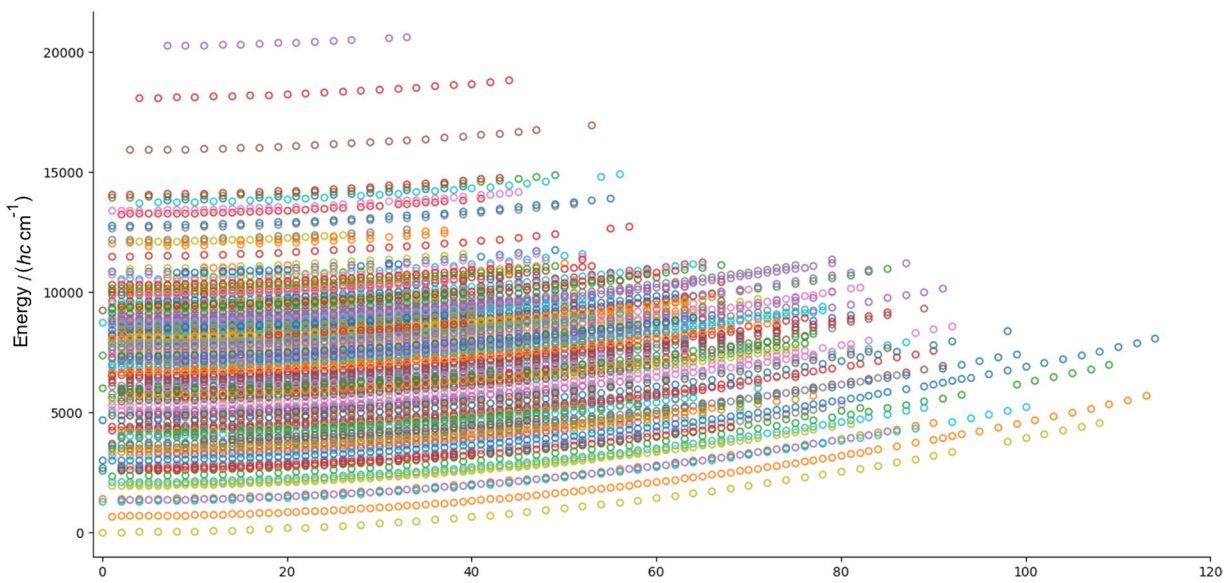


Fig. 3 Pictorial representation of the empirical rovibrational energy levels of the $^{16}\text{O}^{12}\text{C}^{16}\text{O}$ molecule determined in this study, as a function of the rotational quantum number J and the vibrational states (different colors refer to different vibrational states).

Energy level	626M24 energy	CDSD-296 energy	Ames-2021 energy
(0 1 0 0 0 2 e)	1285.408 232(10)	1285.408 208	1285.414 232
(0 1 0 0 0 1 e)	1388.184 211(10)	1388.184 188	1388.186 563
(0 2 0 0 0 3 e)	2548.363 911(1515)	2548.366 693	2548.365 896
(0 2 0 0 0 2 e)	2671.143 110(1118)	2671.142 998	2671.139 583
(0 0 1 1 1 1 e)	3004.012 270(23)	—	—
(0 0 0 0 2 1 e)	4673.325 382(1)	4673.325 381	4673.299 366
(0 1 0 0 2 1 e)	6016.692 186(1000)	6016.690 087	6016.703 928
(0 2 0 0 2 1 e)	7377.705 281(1000)	—	—
(0 3 0 0 2 1 e)	8756.788 201(1000)	—	—
(0 0 0 0 4 1 e)	9246.928 103(5099)	—	—

Table 2. Empirical vibrational band origins of $^{16}\text{O}^{12}\text{C}^{16}\text{O}$ determined in this study (part of the 626M24 dataset) and their counterparts in the CDSD-296²¹ and NASA Ames-2021²² databases. All energy data are in hc cm^{-1} .

'Incorrect HITRAN line position' is used. These 565 HITRAN2020 lines should be reinvestigated and replaced with CDSD-296 or MARVEL positions. (d) When the deviation of the MARVEL position from the CDSD-296 position is larger than 0.005 cm^{-1} , the comment 'Conflict with MARVEL' is used. There are 5110 such cases. They are divided into two groups. First, when both the lower and the upper energy levels are determined by at least three transitions, *i.e.*, the MARVEL prediction is considered to be reliable, '?' is used at the end of the comment. For example, three sources^{76,88,101} measured a line at 3181.915 cm^{-1} , but the CDSD-296 position of this line is 3181.909 cm^{-1} . Most of the cases (4427 occurrences) belong to the second group, where one of the MARVEL energy levels, typically the upper energy level, is defined by only one or two transitions. In this case, '?' is placed at the end of the comment, denoting that it is possible that the experimentally measured line is not reliable. As a point of interest, note that while the initial dataset, "626M24_transitions.txt", contains 816 transitions with uncertainties of less than 10^{-6} cm^{-1} , the number of such transitions in the extended line list, "626M24_line_list.txt", is 2101.

Finally, the file "626M24_MARVEL.exe" is a developer version of the MARVEL code, written in the C++ language. This version of the MARVEL code, distributed with the necessary input files ("626M24_transitions.txt" and "626M24_segments.txt"), was used to generate the numerical data of the 626M24 repository.

Technical Validation

The principal validation of the 626M24 energy levels was performed *via* the MARVEL procedure (see Sec. 2.2). Basically, it involved an elaborate checking of the consistency of the experimentally measured transitions collected, in relation to their assignments, line positions, and uncertainties. Figure 1 shows the final experimental uncertainties of the validated rovibrational measurements of $^{16}\text{O}^{12}\text{C}^{16}\text{O}$ as a function of the transition wavenumber. This figure shows that for $^{16}\text{O}^{12}\text{C}^{16}\text{O}$, one of the spectroscopically most studied molecules, (a) the uncertainties of the experimentally measured transitions cover almost eight orders of magnitude, from 1×10^{-9}

to 10^{-1} cm $^{-1}$, (b) the wavenumber range covered by the experiments is rather limited, only going up to 14 000 cm $^{-1}$, and (c) there are no highly accurate measurements above 7000 cm $^{-1}$.

The global MARVEL analysis resulted in the best rovibrational energy-level dataset, based on the presently available transitions. An important validation of the 626M24 energy values is their comparison with entries in standard databases. Comparison of the predicted line positions of 626M24 with those in the CDSD-296²¹, Ames-2021²², and HITRAN2020²³ line catalogs is particularly important, as it allows additional validation of the energy dataset derived in this study. Furthermore, this comparison might reveal database entries that require further verification and/or modification.

Figure 2 shows the absolute deviations between the MARVEL data and those of CDSD-296 and Ames-2021. The MARVEL data show significantly better agreement with CDSD-296 (with a root-mean-square, rms, deviation of 0.0032 $hc\text{ cm}^{-1}$) than with Ames-2021 (with an rms value of 0.0238 $hc\text{ cm}^{-1}$, which is an order of magnitude higher). This is not surprising, as the CDSD-296 data are semi-empirical in nature. A comparison with the HITRAN2020 data can be found in the file “626M24_line_list.txt”.

Figure 3 shows the empirical rovibrational energy levels of the $^{16}\text{O}^{12}\text{C}^{16}\text{O}$ molecule determined in this study as a function of the rotational quantum number J and the total energy; the vibrational structure can also be seen in the quadratic curves formed as a function of J . Figure 3 shows that the list of rotational energy levels for the ground vibrational state extends up to $J = 108$, but is incomplete, as the $J = 94$ and 96 states are not present in the MARVEL energy levels.

Table 2 lists the vibrational band origins of $^{16}\text{O}^{12}\text{C}^{16}\text{O}$ determined in this study; as $J = 0$ levels only exist for vibrational states with $\ell_2 = 0$, these band origins are only for vibrational states which have $\ell_2 = 0$. It is perhaps surprising to see that there are only nine energies listed there and only four of them have an accuracy better than $1 \times 10^{-3} hc\text{ cm}^{-1}$.

Code availability

The developer version of the MARVEL code, used during the compilation and validation of the 626M24 dataset, is freely available as an OSF repository¹⁸⁴.

Received: 19 December 2024; Accepted: 4 March 2025;

Published online: 29 March 2025

References

- Pearson, P. N. & Palmer, M. R. Atmospheric carbon dioxide concentrations over the past 60 million years. *Nature* **406**, 695–699, <https://doi.org/10.1038/35021000> (2000).
- Romps, D. M., Seeley, J. T. & Edman, J. P. Why the forcing from carbon dioxide scales as the logarithm of its concentration. *J. Climate* **35**, 4027–4047, <https://doi.org/10.1175/JCLI-D-21-0275.1> (2022).
- Shine, K. P. & Perry, G. E. Radiative forcing due to carbon dioxide decomposed into its component vibrational bands. *Q. J. R. Meteorol.* **149**, 1856–1866, <https://doi.org/10.1002/qj.4485> (2023).
- Calvin, K. *et al.* IPCC, 2023: Climate change 2023: Synthesis report. contribution of working groups I, II and III to the sixth assessment report of the intergovernmental panel on climate change [core writing team, H. Lee and J. Romero (eds.)]. IPCC, Geneva, Switzerland, Tech. rep. (2023).
- Baylis-Aguirre, D. K., Creech-Eakman, M. J. & Güth, T. Mid-IR spectra of the M-type Mira variable R Tri observed with the Spitzer IRS. *Mon. Not. Roy. Astron. Soc.* **493**, 807–814, <https://doi.org/10.1093/mnras/staa322> (2020).
- Fonfria, J. P., Montiel, E. J., Cernicharo, J., DeWitt, C. N. & Richter, M. J. Detection of infrared fluorescence of carbon dioxide in R Leonis with SOFIA/EXES. *Astron. Astrophys.* **643**, L15, <https://doi.org/10.1051/0004-6361/202039547> (2020).
- Gilli, G. *et al.* Limb observations of CO₂ and CO non-LTE emissions in the Venus atmosphere by VIRTIS/Venus Express. *J. Geophys. Res.-Planets* **114**, E00B29, <https://doi.org/10.1029/2008JE003112> (2009).
- Snels, M., Stefani, S., Grassi, D., Piccioni, G. & Adriani, A. Carbon dioxide opacity of the Venus’ atmosphere. *Planet Space Sci.* **103**, 347–354, <https://doi.org/10.1016/j.pss.2014.08.002> (2014).
- Trokhimovskiy, A. *et al.* First observation of the magnetic dipole CO₂ main isotopologue absorption band at 3.3 μm in the atmosphere of Mars by the ExoMars Trace Gas Orbiter ACS instrument. *Astron. Astrophys.* **639**, A142, <https://doi.org/10.1051/0004-6361/202038134> (2020).
- Swain, M. R. *et al.* Molecular signatures in the near-infrared dayside spectrum of HD 189733b. *Astrophys. J. Lett.* **690**, L114–L117, <https://doi.org/10.1088/0004-637X/690/2/L114> (2009).
- Ahrer, E.-M. *et al.* Identification of carbon dioxide in an exoplanet atmosphere. *Nature* **614**, 649–652, <https://doi.org/10.1038/s41586-022-05269-w> (2023).
- Boonman, A. M. S. *et al.* Gas-phase CO₂, C₂H₂, and HCN toward Orion-KL*. *Astron. Astrophys.* **399**, 1047–1061, <https://doi.org/10.1051/0004-6361/20021799> (2003).
- Boonman, A. M. S., van Dishoeck, E. F., Lahuis, F. & Doty, S. D. Gas-phase CO₂ toward massive protostars. *Astron. Astrophys.* **399**, 1063–1072, <https://doi.org/10.1051/0004-6361/20021868> (2003).
- Hobbs, J. M. *et al.* Spectroscopic uncertainty impacts on OCO-2/3 retrievals of XCO₂. *J. Quant. Spectrosc. Radiat. Transf.* **257**, 107360, <https://doi.org/10.1016/j.jqsrt.2020.107360> (2020).
- Noel, S. *et al.* Greenhouse gas retrievals for the CO2M mission using the FOCAL method: first performance estimates. *Atmos. Meas. Tech.* **17**, 2317–2334, <https://doi.org/10.5194/amt-17-2317-2024> (2024).
- Laughner, J. L. *et al.* The Total Carbon Column Observing Network’s GGG2020 data version. *Earth Sys. Sci. Data* **16**, 2197–2260, <https://doi.org/10.5194/essd-16-2197-2024> (2024).
- Ageev, V. G. & Nikiforova, O. Y. Optoacoustic determination of carbon dioxide concentration in exhaled breath in various human diseases. *J. Appl. Spectrosc.* **83**, 820–825, <https://doi.org/10.1007/s10812-016-0369-z> (2016).
- Evseev, V., Fateev, A. & Clausen, S. High-resolution transmission measurements of CO₂ at high temperatures for industrial applications. *J. Quant. Spectrosc. Radiat. Transf.* **113**, 2222–2233, <https://doi.org/10.1016/j.jqsrt.2012.07.015> (2012).
- Du, Y., Tsankov, T. V., Luggenhölscher, D. & Czarnetzki, U. Time evolution of CO₂ ro-vibrational excitation in a nanosecond discharge measured with laser absorption spectroscopy. *J. Phys.D-Appl. Phys.* **54**, 365201, <https://doi.org/10.1088/1361-6463/ac03e7> (2021).
- Snoeckx, R. & Bogaerts, A. Plasma technology - a novel solution for CO₂ conversion? *Chem. Soc. Rev.* **46**, 5805–5863, <https://doi.org/10.1039/c6cs00066e> (2017).

21. Tashkun, S. A., Perevalov, V. I., Gamache, R. R. & Lamouroux, J. CDSD-296, high-resolution carbon dioxide spectroscopic databank: An update. *J. Quant. Spectrosc. Radiat. Transf.* **228**, 124–131, <https://doi.org/10.1016/j.jqsrt.2019.03.001> (2019).
22. Huang, X., Schwenke, D. W., Freedman, R. S. & Lee, T. J. Ames-2021 CO₂ dipole moment surface and IR line lists: Toward 0.1% uncertainty for CO₂ IR intensities. *J. Phys. Chem. A* **126**, 5940–5964, <https://doi.org/10.1021/acs.jpca.2c01291> (2022).
23. Gordon, I. E. *et al.* The HITRAN2020 molecular spectroscopic database. *J. Quant. Spectrosc. Radiat. Transf.* **277**, 107949, <https://doi.org/10.1016/j.jqsrt.2021.107949> (2022).
24. Yurchenko, S. N., Mellor, T. M., Freedman, R. S. & Tennyson, J. ExoMol molecular line lists XXXIX: Ro-vibrational molecular line list for CO₂. *Mon. Not. Roy. Astron. Soc.* **496**, 5282–5291, <https://doi.org/10.1093/mnras/staa1874> (2020).
25. Alatoom, D. *et al.* MARVEL analysis of high-resolution rovibrational spectra of ¹⁶O¹²C¹⁸O. *J. Comput. Chem.* **45**, 2558–2573, <https://doi.org/10.1002/jcc.27453> (2024).
26. Ibrahim, M. T. I. *et al.* MARVEL analysis of high-resolution rovibrational spectra of ¹⁶O¹³C¹⁶O. *J. Comput. Chem.* **45**, 969–984, <https://doi.org/10.1002/jcc.27266> (2024).
27. Azzam, A. A. A., Tennyson, J., Yurchenko, S. N., Furtenbacher, T. & Császár, A. G. MARVEL analysis of high-resolution rovibrational spectra of ¹⁶O¹³C¹⁸O. *J. Comput. Chem.* **46**, e27541, <https://doi.org/10.1002/jcc.27541> (2025).
28. Azzam, A. A. A. *et al.* MARVEL analysis of high-resolution rovibrational spectra of the ¹⁸O¹²C¹⁸O, ¹⁷O¹²C¹⁸O, and ¹⁸O¹³C¹⁸O isotopologues of carbon dioxide. *J. Mol. Spectrosc.* **405**, 111947, <https://doi.org/10.1016/j.jms.2024.111947> (2024).
29. Császár, A. G., Czakó, G., Furtenbacher, T. & Mátyus, E. An active database approach to complete rotational-vibrational spectra of small molecules. *Annu. Rep. Comput. Chem.* **3**, 155–176, [https://doi.org/10.1016/S1574-1400\(07\)03009-5](https://doi.org/10.1016/S1574-1400(07)03009-5) (2007).
30. Furtenbacher, T., Császár, A. G. & Tennyson, J. MARVEL: measured active rotational-vibrational energy levels. *J. Mol. Spectrosc.* **245**, 115–125, <https://doi.org/10.1016/j.jms.2007.07.005> (2007).
31. Furtenbacher, T. & Császár, A. G. MARVEL: measured active rotational-vibrational energy levels. II. Algorithmic improvements. *J. Quant. Spectrosc. Radiat. Transf.* **113**, 929–935, <https://doi.org/10.1016/j.jqsrt.2012.01.005> (2012).
32. Tennyson, J., Furtenbacher, T., Yurchenko, S. N. & Császár, A. G. Empirical rovibrational energy levels for nitrous oxide. *J. Quant. Spectrosc. Radiat. Transf.* **316**, 108902, <https://doi.org/10.1016/j.jqsrt.2024.108902> (2024).
33. Császár, A. G. & Furtenbacher, T. Spectroscopic networks. *J. Mol. Spectrosc.* **266**, 99–103, <https://doi.org/10.1016/j.jms.2011.03.031> (2011).
34. Furtenbacher, T. & Császár, A. G. The role of intensities in determining characteristics of spectroscopic networks. *J. Mol. Struct.* **1009**, 123–129, <https://doi.org/10.1016/j.molstruc.2011.10.057> (2012).
35. Tennyson, J. *et al.* The 2024 release of the ExoMol database: molecular line lists for exoplanet and other hot atmospheres. *J. Quant. Spectrosc. Radiat. Transf.* **326**, 109083, <https://doi.org/10.1016/j.jqsrt.2024.109083> (2024).
36. Martin, P. E. & Barker, E. F. The infrared absorption spectrum of carbon dioxide. *Phys. Rev.* **41**, 291–303, <https://doi.org/10.1103/PhysRev.41.291> (1932).
37. Nielsen, A. H. & Yao, Y. T. The analysis of the vibration-rotation band ω_3 for ¹²C¹⁶O₂ and ¹³C¹⁶O₂. *Phys. Rev.* **68**, 173–180, <https://doi.org/10.1103/PhysRev.68.173> (1945).
38. Goldberg, L., Mohler, O. C., McMath, R. R. & Pierce, A. K. Carbon dioxide in the infra-red solar spectrum. *Phys. Rev.* **76**, 1848–1858, <https://doi.org/10.1103/PhysRev.76.1848> (1949).
39. Herzberg, G. & Herzberg, L. Rotation-vibration spectra of diatomic and simple polyatomic molecules with long absorbing paths XI. The spectrum of carbon dioxide (CO₂) below 1.25 μm. *J. Opt. Soc. Am.* **43**, 1037–1044, <https://doi.org/10.1364/JOSA.43.001037> (1953).
40. Rossmann, K., Rao, K. N. & Nielsen, H. H. Infrared spectrum and molecular constants of carbon dioxide. Part I. ν_2 of ¹²C¹⁶O₂ at 15 μ. *J. Chem. Phys.* **24**, 103–105, <https://doi.org/10.1063/1.1700807> (1956).
41. Madden, R. P. A high-resolution study of CO₂ absorption spectra between 15 and 18 microns. *J. Chem. Phys.* **35**, 2083–2097, <https://doi.org/10.1063/1.1732212> (1961).
42. Plyler, E. K., Tidwell, E. D. & Benedict, W. S. Absorption bands of carbon dioxide from 2.8–4.2 μ. *J. Opt. Soc. Am.* **52**, 1017–1022, <https://doi.org/10.1364/JOSA.52.001017> (1962).
43. Gordon, H. R. & McCubbin, T. K. The 15-micron bands of ¹²C¹⁶O₂. *J. Mol. Spectrosc.* **18**, 73–82, [https://doi.org/10.1016/0022-2852\(65\)90063-9](https://doi.org/10.1016/0022-2852(65)90063-9) (1965).
44. Gordon, H. R. The infrared spectrum of CO₂ in the 2.8 and 15 micron regions, Ph.D. thesis, The Pennsylvania State University <https://www.proquest.com/openview/59dcaa567b3cb6b908786d3699a70cc9/1?pq-origsite=gscholar&cbl=18750&diss=y> (1965).
45. Gordon, H. R. & McCubbin, T. K. The 2.8-micron bands of CO₂. *J. Mol. Spectrosc.* **19**, 137–154, [https://doi.org/10.1016/0022-2852\(66\)90237-2](https://doi.org/10.1016/0022-2852(66)90237-2) (1966).
46. Hartmann, B. & Kleman, B. Laser lines from CO₂ in the 11–18 micron region. *Can. J. Phys.* **44**, 1609–1612, <https://doi.org/10.1139/p66-134> (1966).
47. Hahn, Y. H. The absorption and emission spectra of carbon-dioxide at 4.3 microns, Ph.D. thesis, The Pennsylvania State University <https://www.proquest.com/openview/074bf2696a7b47d2793ca1d620a02193/1?pq-origsite=gscholar&cbl=18750&diss=y> (1967).
48. Oberly, R., Rao, K. N., Hahn, Y. H. & McCubbin, T. K. Bands of carbon dioxide in the region of 4.3 microns. *J. Mol. Spectrosc.* **25**, 138–165, [https://doi.org/10.1016/0022-2852\(68\)80002-5](https://doi.org/10.1016/0022-2852(68)80002-5) (1968).
49. Gray Young, L. D., Young, A. T. & Schorn, R. A. Improved constants for the 7820 Å and 7883 Å bands of CO₂. *J. Quant. Spectrosc. Radiat. Transfer* **10**, 1291–1300, [https://doi.org/10.1016/0022-4073\(70\)90011-7](https://doi.org/10.1016/0022-4073(70)90011-7) (1970).
50. Blaney, T. G. *et al.* Absolute frequency measurement of the R(12) Transition of CO₂ at 9.3 μm. *Nature* **244**, 504–504, <https://doi.org/10.1038/244504a0> (1973).
51. Evenson, K. M., Wells, J. S., Petersen, F. R., Danielson, B. L. & Day, G. W. Accurate frequencies of molecular transitions used in laser stabilization: the 3.39-μm transition in CH₄ and the 9.33- and 10.18-μm transitions in CO₂. *Appl. Phys. Lett.* **22**, 192–195, <https://doi.org/10.1063/1.1654607> (1973).
52. Schiffner, G. Improved determination of accurate CO₂ laser transition frequencies and their standard deviation. *Opto-Electronics* **5**, 411–413, <https://doi.org/10.1007/bf01418076> (1973).
53. McCubbin, T. K., Pliva, J., Pulfrey, R., Telfair, W. & Todd, T. The emission spectrum of ¹²C¹⁶O₂ from 4.2 to 4.7 microns. *J. Mol. Spectrosc.* **49**, 136–156, [https://doi.org/10.1016/0022-2852\(74\)90103-9](https://doi.org/10.1016/0022-2852(74)90103-9) (1974).
54. Toth, R. A. Wavenumbers, strengths, and self-broadened widths of CO₂ at 3 μm. *J. Mol. Spectrosc.* **53**, 1–14, [https://doi.org/10.1016/0022-2852\(74\)90256-2](https://doi.org/10.1016/0022-2852(74)90256-2) (1974).
55. Dupre-Maquaire, J. & Pinson, P. Emission spectrum of CO₂ in the 9.6 μm region. *J. Mol. Spectrosc.* **62**, 181–191, [https://doi.org/10.1016/0022-2852\(76\)90348-9](https://doi.org/10.1016/0022-2852(76)90348-9) (1976).
56. Reid, J. & Siemsen, K. New CO₂ laser bands in the 9–11-μm wavelength region. *Appl. Phys. Lett.* **29**, 250–251, <https://doi.org/10.1063/1.89033> (1976).
57. Monchal, J. P., Kelly, M. J., Thomas, J. E., Kurnit, N. A. & Javan, A. Accurate wavelength measurement of P-branch transitions of the 01¹ – [11⁰, 03⁰] band of ¹²C¹⁶O₂ and determination of the band parameters. *J. Mol. Spectrosc.* **64**, 491–494, [https://doi.org/10.1016/0022-2852\(77\)90233-8](https://doi.org/10.1016/0022-2852(77)90233-8) (1977).
58. Nereson, N. G. & Flicker, H. Wavenumber measurement of weak CO₂ laser lines around 10.6 μm. *Opt. Commun.* **23**, 171–176, [https://doi.org/10.1016/0030-4018\(77\)90299-1](https://doi.org/10.1016/0030-4018(77)90299-1) (1977).
59. Whitford, B. G., Siemsen, K. J. & Reid, J. Heterodyne frequency measurements of CO₂ laser hot-band transitions. *Opt. Commun.* **22**, 261–264, [https://doi.org/10.1016/S0030-4018\(97\)90004-3](https://doi.org/10.1016/S0030-4018(97)90004-3) (1977).

60. Siemens, K. J. & Whitford, B. G. Heterodyne frequency measurements of CO₂ laser sequence-band transitions. *Opt. Commun.* **22**, 11–16, [https://doi.org/10.1016/0030-4018\(77\)90235-8](https://doi.org/10.1016/0030-4018(77)90235-8) (1977).
61. Arcas, P. & Arié, E. Absorption spectrum of CO₂ in the 4.82-μm region. *J. Mol. Spectrosc.* **70**, 134–142, [https://doi.org/10.1016/0022-2852\(78\)90015-2](https://doi.org/10.1016/0022-2852(78)90015-2) (1978).
62. Baldacci, A., Devi, V. M., Chen, D.-W., Rao, K. N. & Fridovich, B. Absorption spectrum of carbon dioxide at 4.3 μm. *J. Mol. Spectrosc.* **70**, 143–159, [https://doi.org/10.1016/0022-2852\(78\)90016-4](https://doi.org/10.1016/0022-2852(78)90016-4) (1978).
63. Roney, P. L., Findlay, F. D., Buijs, H. L., Cann, M. W. P. & Nicholls, R. W. Carbon dioxide spectral line frequencies for the 43-μm region. *Appl. Opt.* **17**, 2599, <https://doi.org/10.1364/AO.17.002599> (1978).
64. Freed, C., Bradley, L. & O'Donnell, R. Absolute frequencies of lasing transitions in seven CO₂ isotopic species. *IEEE J. Quantum Electron.* **16**, 1195–1206, <https://doi.org/10.1109/jqe.1980.1070392> (1980).
65. Guelachvili, G. High-resolution Fourier spectra of carbon dioxide and three of its isotopic species near 4.3 μm. *J. Mol. Spectrosc.* **79**, 72–83, [https://doi.org/10.1016/0022-2852\(80\)90293-3](https://doi.org/10.1016/0022-2852(80)90293-3) (1980).
66. Maillard, J. P., Cuisenier, M., Arcas, P., Arié, E. & Amiot, C. Infrared spectrum and molecular constants of CO₂ in the 1.4–1.7 μm atmospheric window by very high resolution Fourier transform spectroscopy. *Can. J. Phys.* **58**, 1560–1569, <https://doi.org/10.1139/p80-205> (1980).
67. Paso, R., Kauppinen, J. & Anttila, R. Infrared spectrum of CO₂ in the region of the bending fundamental ν₂. *J. Mol. Spectrosc.* **79**, 236–253, [https://doi.org/10.1016/0022-2852\(80\)90304-5](https://doi.org/10.1016/0022-2852(80)90304-5) (1980).
68. Pine, A. S. & Guelachvili, G. R-branch head of the ν₃ band of CO₂ at elevated temperatures. *J. Mol. Spectrosc.* **79**, 84–89, [https://doi.org/10.1016/0022-2852\(80\)90294-5](https://doi.org/10.1016/0022-2852(80)90294-5) (1980).
69. Baillly, D., Farrenq, R., Guelachvili, G. & Rossetti, C. ¹²C¹⁶O₂ analysis of emission Fourier spectra in the 4.5-μm region: Rovibrational transitions 0ν₂'ν₃ – 0ν₂'(ν₃ – 1), ν₂ = ℓ. *J. Mol. Spectrosc.* **90**, 74–105, [https://doi.org/10.1016/0022-2852\(81\)90334-9](https://doi.org/10.1016/0022-2852(81)90334-9) (1981).
70. Kauppinen, J., Jolma, K. & Horneman, V. M. New wave-number calibration tables for H₂O, CO₂, and OCS lines between 500 and 900 cm⁻¹. *Appl. Opt.* **21**, 3332–6, <https://doi.org/10.1364/AO.21.003332> (1982).
71. Arcas, P., Arié, E., Cuisenier, M. & Maillard, J. P. The infrared spectrum and molecular constants of CO₂ in the 2 μm region. *Can. J. Phys.* **61**, 857–866, <https://doi.org/10.1139/p83-105> (1983).
72. Jolma, K., Kauppinen, J. & Horneman, V. M. Vibration-rotation bands of CO₂ and OCS in the region 540–890 cm⁻¹. *J. Mol. Spectrosc.* **101**, 300–305, [https://doi.org/10.1016/0022-2852\(83\)90135-2](https://doi.org/10.1016/0022-2852(83)90135-2) (1983).
73. Petersen, F. R., Beaty, E. C. & Pollock, C. R. Improved rovibrational constants and frequency tables for the normal laser bands of ¹²C¹⁶O₂. *J. Mol. Spectrosc.* **102**, 112–122, [https://doi.org/10.1016/0022-2852\(83\)90231-X](https://doi.org/10.1016/0022-2852(83)90231-X) (1983).
74. Devi, V. M., Rinsland, C. P. & Benner, D. C. Absolute intensity measurements of CO₂ bands in the 2395–2680-cm⁻¹ region. *Appl. Opt.* **23**, 4067, <https://doi.org/10.1364/AO.23.004067> (1984).
75. Rinsland, C. P. & Benner, D. C. Absolute intensities of spectral lines in carbon dioxide bands near 2050 cm⁻¹. *Appl. Opt.* **23**, 4523–4528, <https://doi.org/10.1364/AO.23.004523> (1984).
76. Rinsland, C. P. *et al.* Atlas of high resolution infrared spectra of carbon dioxide. *Appl. Opt.* **23**, 2051–2052, <https://doi.org/10.1364/AO.23.002051> (1984).
77. Petersen, F. R., Wells, J. S., Siemsen, K. J., Robinson, A. M. & Maki, A. G. Heterodyne frequency measurements and analysis of CO₂ laser hot band transitions. *J. Mol. Spectrosc.* **105**, 324–330, [https://doi.org/10.1016/0022-2852\(84\)90222-4](https://doi.org/10.1016/0022-2852(84)90222-4) (1984).
78. Benner, D. C. & Rinsland, C. P. Identification and intensities of the “forbidden” 3ν₂³ band of ¹²C¹⁶O₂. *J. Mol. Spectrosc.* **112**, 18–25, [https://doi.org/10.1016/0022-2852\(85\)90187-0](https://doi.org/10.1016/0022-2852(85)90187-0) (1985).
79. Brown, L. R. & Toth, R. A. Comparison of the frequencies of NH₃, CO₂, H₂O, N₂O, CO, and CH₄ as infrared calibration standards. *J. Opt. Soc. Am. B* **2**, 842–856, <https://doi.org/10.1364/JOSAB.2.000842> (1985).
80. Rinsland, C. P., Benner, D. C. & Devi, V. M. Measurements of absolute line intensities in carbon dioxide bands near 5.2 μm. *Appl. Opt.* **24**, 1644–1650, <https://doi.org/10.1364/AO.24.001644> (1985).
81. Bradley, L., Soohoo, K. & Freed, C. Absolute frequencies of lasing transitions in nine CO₂ isotopic species. *IEEE J. Quantum Electron.* **22**, 234–267, <https://doi.org/10.1109/JQE.1986.1072967> (1986).
82. Chardonnet, C., van Lerberghe, A. & Bordé, C. J. Absolute frequency determination of super-narrow CO₂ saturation peaks observed in an external absorption cell. *Opt. Commun.* **58**, 333–337, [https://doi.org/10.1016/0030-4018\(86\)90239-7](https://doi.org/10.1016/0030-4018(86)90239-7) (1986).
83. Esplin, M. P. & Rothman, L. S. Spectral measurements of high-temperature isotopic carbon dioxide in the 4.5- and 2.8 μm regions. *J. Mol. Spectrosc.* **116**, 351–363, [https://doi.org/10.1016/0022-2852\(86\)90132-3](https://doi.org/10.1016/0022-2852(86)90132-3) (1986).
84. Esplin, M. P. *et al.* Carbon dioxide line positions in the 2.8 and 4.3 micron regions at 800 Kelvin, Tech. Rep. AFGL-TR-86-0046, Utah State University <https://apps.dtic.mil/sti/citations/ADA173808> (1986).
85. Guelachvili, G., Rao, K. R. Handbook of Infrared Standards, Academic Press, (1986).
86. Rinsland, C. P., Benner, D. C. & Devi, V. M. Absolute line intensities in CO₂ bands near 4.8 μm. *Appl. Opt.* **25**, 1204–1214, <https://doi.org/10.1364/AO.25.001204> (1986).
87. Blanquet, G., Walrand, J. & Teffo, J. L. Frequency diode laser measurement of a very weak Q branch of CO₂ near 864 cm⁻¹. *Appl. Opt.* **27**, 2098–2099, <https://doi.org/10.1364/ao.27.002098> (1988).
88. Benner, D. C., Devi, V. M., Rinsland, C. P. & Ferry-Leeper, P. S. Absolute intensities of CO₂ lines in the 3140–3410-cm⁻¹ spectral region. *Appl. Opt.* **27**, 1588–1597, <https://doi.org/10.1364/AO.27.001588> (1988).
89. Ouazzany, Y., Boquillon, J. P. & Schröter, H. W. High resolution CARS spectrum and analysis of the ν₁ band Q-branch of carbon dioxide. *Mol. Phys.* **63**, 769–777, <https://doi.org/10.1080/00268978800100551> (1988).
90. Hamdouni, A. & Dana, V. Absolute line intensities in the 20002 ← 11102 and 12201 ← 03301 bands of ¹²C¹⁶O₂. *Appl. Opt.* **29**, 1570–1572, <https://doi.org/10.1364/AO.29.001570> (1990).
91. Giver, L. P. & Chackerian, C. Rovibrational intensities for the (31¹0)_{IV} ← (00⁰0) band of ¹²C¹⁶O₂ at 4416 cm⁻¹. *J. Mol. Spectrosc.* **148**, 80–85, [https://doi.org/10.1016/0022-2852\(91\)90036-a](https://doi.org/10.1016/0022-2852(91)90036-a) (1991).
92. Groh, A., Goddon, D., Schneider, M., Zimmermann, W. & Urban, W. Sub-doppler heterodyne frequency measurements on the CO₂ 10011–00001 vibrational band: New reference lines near 3714 cm⁻¹. *J. Mol. Spectrosc.* **146**, 161–168, [https://doi.org/10.1016/0022-2852\(91\)90379-O](https://doi.org/10.1016/0022-2852(91)90379-O) (1991).
93. Baillly, D. ¹²C¹⁶O₂ in emission in the 4.5-μm region: Some more rovibrational transitions ν₁ν₂'ν₃ ← ν₁'ν₂(ν₃ – 1) occurring between very few populated levels. *J. Mol. Spectrosc.* **166**, 1–11, <https://doi.org/10.1006/jmsp.1994.1166> (1994).
94. Maki, A. G., Chou, C. C., Evenson, K. M., Zink, L. R. & Shy, J. T. Improved molecular constants and frequencies for the CO₂ laser from new high-J regular and hot-band frequency measurements. *J. Mol. Spectrosc.* **167**, 211–224, <https://doi.org/10.1006/jmsp.1994.1227> (1994).
95. Chou, C. C. *et al.* Frequency measurements and molecular constants of CO₂ 00⁰2-[10⁰1,02⁰1]_{I,II} sequence band transitions. *J. Mol. Spectrosc.* **172**, 233–242, <https://doi.org/10.1006/jmsp.1995.1171> (1995).
96. Steyert, D. W., Weber, M., Sirota, J. M. & Reuter, D. C. Absolute intensities for the Q-branch of the 4ν₂² ← 3ν₂³ (581.776 cm⁻¹) band in carbon dioxide. *J. Quant. Spectrosc. Rad. Transf.* **54**, 815–818, [https://doi.org/10.1016/0022-4073\(95\)00101-p](https://doi.org/10.1016/0022-4073(95)00101-p) (1995).
97. Baillly, D., Camy-Peyret, C. & Lanquetin, R. Temperature measurement in flames through CO₂ and CO emission: New highly excited levels of CO₂. *J. Mol. Spectrosc.* **182**, 10–17, <https://doi.org/10.1006/jmsp.1996.7205> (1997).

98. Bernard, V., Nogues, G., Daussy, C., Constantin, L. & Chardonnet, C. CO₂ laser stabilized on narrow saturated absorption resonances of CO₂, improved absolute frequency measurements. *Metrologia* **34**, 313, <https://doi.org/10.1088/0026-1394/34/4/4> (1997).
99. Bailly, D. ¹²C¹⁶O₂ in emission in the 4.5-μm region: Transitions $\nu_1 \nu_2 \nu_3 \leftarrow \nu_1 \nu_2 (\nu_3 - 1)$ with $(2\nu_1 + \nu_2) = 6$ occurring between highly excited vibrational states. *J. Mol. Spectrosc.* **192**, 257–262, <https://doi.org/10.1006/jmsp.1998.7667> (1998).
100. Bailly, D., Tashkun, S. A., Perevalov, V. I., Teffo, J. L. & Arcas, P. H. CO₂ emission in the 4-μm region: The $(2^11)_3 \leftarrow (2^10)_3$ transition revisited. *J. Mol. Spectrosc.* **190**, 1–6, <https://doi.org/10.1006/jmsp.1998.7534> (1998).
101. Devi, V. M., Benner, D. C., Rinsland, C. P. & Smith, M. A. H. Absolute rovibrational intensities of ¹²C¹⁶O₂ absorption bands in the 3090–3850 cm⁻¹ spectral region. *J. Quant. Spectrosc. Rad. Transf.* **60**, 741–770, [https://doi.org/10.1016/s0022-4073\(98\)00080-6](https://doi.org/10.1016/s0022-4073(98)00080-6) (1998).
102. Frech, B. *et al.* Frequency measurements of saturated-fluorescence-stabilized CO₂ laser lines: comparison with an OsO₄-stabilized CO₂ laser standard. *Appl. Phys. B* **67**, 217–221, <https://doi.org/10.1007/s003400050496> (1998).
103. Bailly, D., Tashkun, S., Perevalov, V. I., Teffo, J. L. & Arcas, P. Flame spectra of CO₂ in the 3-μm region. *J. Mol. Spectrosc.* **197**, 114–119, <https://doi.org/10.1006/jmsp.1999.7883> (1999).
104. Campargue, A., Bailly, D., Teffo, J. L., Tashkun, S. A. & Perevalov, V. I. The $\nu_1 + 5\nu_3$ dyad of ¹²CO₂ and ¹³CO₂. *J. Mol. Spectrosc.* **193**, 204–212, <https://doi.org/10.1006/jmsp.1998.7718> (1999).
105. Acef, O., Michaud, F. & Rovera, G. V. Accurate determination of OsO₄ absolute frequency grid at 28/29 THz. *IEEE Trans. Instr. Meas.* **48**, 567–570 (1999).
106. Predoi-Cross, A., Luo, C., Berman, R., Drummond, J. R. & May, A. D. Line strengths, self-broadening, and line mixing in the $200 \leftarrow 01^10 (\Sigma \leftarrow \Pi)$ Q branch of carbon dioxide. *J. Chem. Phys.* **112**, 8367–8377, <https://doi.org/10.1063/1.481480> (2000).
107. Tashkun, S. A. *et al.* ¹³C¹⁶O₂: Global treatment of vibrational-rotational spectra and first observation of the $2\nu_1 + 5\nu_3$ and $\nu_1 + 2\nu_2 + 5\nu_3$ absorption bands. *J. Mol. Spectrosc.* **200**, 162–176, <https://doi.org/10.1006/jmsp.2000.8057> (2000).
108. Teffo, J.-L. *et al.* Line intensities of ¹²C¹⁶O₂ in the 1.2–1.4 μm spectral region. *J. Mol. Spectrosc.* **201**, 249–255, <https://doi.org/10.1006/jmsp.2000.8092> (2000).
109. Chou, C.-C., Lin, T. & Shy, J.-T. Wavenumber measurements of CO₂ transitions in 1.5-μm atmospheric window using an external-cavity diode laser. *J. Mol. Spectrosc.* **205**, 122–127, <https://doi.org/10.1006/jmsp.2000.8242> (2001).
110. Weirauch, G. & Campargue, A. Spectroscopy and intensity measurements of the $3\nu_1 + 3\nu_3$ tetrad of ¹²CO₂ and ¹³CO₂. *J. Mol. Spectrosc.* **207**, 263–268, <https://doi.org/10.1006/jmsp.2001.8342> (2001).
111. Vander Auwera, J., El Hachoutki, R. & Brown, L. R. Absolute line wavenumbers in the near infrared: ¹²C₂H₂ and ¹²C¹⁶O₂. *Mol. Phys.* **100**, 3563–3576, <https://doi.org/10.1080/00268970210162880> (2002).
112. Ding, Y., Bertseva, E. & Campargue, A. Note: The $2\nu_1 + 3\nu_3$ triad of ¹²CO₂. *J. Mol. Spectrosc.* **212**, 219–222, <https://doi.org/10.1006/jmsp.2002.8553> (2002).
113. Devi, V. M., Benner, D. C., Smith, M. A. H. & Rinsland, C. P. Nitrogen broadening and shift coefficients in the 4.2–4.5 micron bands of CO₂. *J. Quant. Spectrosc. Rad. Transf.* **76**, 289–307 (2003).
114. Giver, L. P., Brown, L. R., Chackerian, C. & Freedman, R. S. The rovibrational intensities of five absorption bands of between 5218 and 5349 cm⁻¹. *J. Quant. Spectrosc. Rad. Transf.* **78**, 417–436, [https://doi.org/10.1016/s0022-4073\(02\)00277-7](https://doi.org/10.1016/s0022-4073(02)00277-7) (2003).
115. Miller, C. E. & Brown, L. R. Near infrared spectroscopy of carbon dioxide I. ¹⁶O¹²C¹⁶O line positions. *J. Mol. Spectrosc.* **228**, 329–354, <https://doi.org/10.1016/j.jms.2003.11.001> (2004).
116. André, F., Perrin, M. Y. & Taine, J. FTIR measurements of ¹²C¹⁶O₂ line positions and intensities at high temperature in the 3700–3750 cm⁻¹ spectral region. *J. Mol. Spectrosc.* **228**, 187–205, <https://doi.org/10.1016/j.jms.2004.07.004> (2004).
117. Amy-Klein, A., Vigué, H. & Chardonnet, C. Absolute frequency measurement of ¹²C¹⁶O₂ laser lines with a femtosecond laser comb and new determination of the ¹²C¹⁶O₂ molecular constants and frequency grid. *J. Mol. Spectrosc.* **228**, 206–212, <https://doi.org/10.1016/j.jms.2004.07.005> (2004).
118. Ding, Y., Campargue, A., Bertseva, E., Tashkun, S. & Perevalov, V. I. Highly sensitive absorption spectroscopy of carbon dioxide by ICLAS-VeCSEL between 8800 and 9530 cm⁻¹. *J. Mol. Spectrosc.* **231**, 117–123, <https://doi.org/10.1016/j.jms.2004.12.008> (2005).
119. Garnache, A., Liu, A., Cerutti, L. & Campargue, A. Intracavity laser absorption spectroscopy with a vertical external cavity surface emitting laser at 2.3 μm: Application to water and carbon dioxide. *Chem. Phys. Lett.* **416**, 22–27, <https://doi.org/10.1016/j.cplett.2005.09.028> (2005).
120. Lucchesini, A. & Gozzini, S. Diode laser overtone spectroscopy of CO₂ at 780 nm. *J. Quant. Spectrosc. Radiat. Transf.* **96**, 289–299, <https://doi.org/10.1016/j.jqsrt.2005.03.005> (2005).
121. Mazzotti, D., Cancio, P., Giusfredi, G., De Natale, P. & Prevedelli, M. Frequency-comb-based absolute frequency measurements in the mid-infrared with a difference-frequency spectrometer. *Opt. Lett.* **30**, 997, <https://doi.org/10.1364/ol.30.000997> (2005).
122. Majcherova, Z. *et al.* High-sensitivity CW-cavity ringdown spectroscopy of ¹²CO₂ near 1.5 μm. *J. Mol. Spectrosc.* **230**, 1–21, <https://doi.org/10.1016/j.jms.2004.09.011> (2005).
123. Shao, J. *et al.* Highly sensitive diode laser absorption measurements of CO₂ near 1.57 μm at room temperature. *Opt. Appl.* **XXXV**, 49–57 (2005).
124. Wang, L., Perevalov, V. I., Tashkun, S. A., Liu, A. W. & Hu, S. M. Absorption spectra of ¹²C¹⁶O₂ and ¹³C¹⁶O₂ near 1.05 μm. *J. Mol. Spectrosc.* **233**, 297–300, <https://doi.org/10.1016/j.jms.2005.07.008> (2005).
125. Perevalov, B. V. *et al.* CW-cavity ringdown spectroscopy of carbon dioxide isotopologues near 1.5 μm. *J. Mol. Spectrosc.* **238**, 241–255, <https://doi.org/10.1016/j.jms.2006.05.009> (2006).
126. Toth, R. A., Brown, L. R., Miller, C. E., Devi, V. M. & Benner, D. C. Line strengths of ¹²C¹⁶O₂: 4550–7000 cm⁻¹. *J. Mol. Spectrosc.* **239**, 221–242, <https://doi.org/10.1016/j.jms.2006.08.001> (2006).
127. Horneman, V.-M. High accurate peak positions for calibration purposes with the lowest fundamental bands ν_2 of N₂O and CO₂. *J. Mol. Spectrosc.* **241**, 45–50, <https://doi.org/10.1016/j.jms.2006.10.014> (2007).
128. Lucchesini, A. & Gozzini, S. Diode laser spectroscopy of CO₂ at 790 nm. *J. Quant. Spectrosc. Rad. Transf.* **103**, 74–82, <https://doi.org/10.1016/j.jqsrt.2006.06.009> (2007).
129. Borri, S. *et al.* Lamb-dip-locked quantum cascade laser for comb-referenced IR absolute frequency measurements. *Opt. Expr.* **16**, 11637, <https://doi.org/10.1364/oe.16.011637> (2008).
130. Perevalov, B. V., Kassi, S., Perevalov, V. I., Tashkun, S. A. & Campargue, A. High sensitivity CW-CRDS spectroscopy of ¹²C¹⁶O₂, ¹⁶O¹²C¹⁷O and ¹⁶O¹²C¹⁸O between 5851 and 7045 cm⁻¹: Line positions analysis and critical review of the current databases. *J. Mol. Spectrosc.* **252**, 143–159, <https://doi.org/10.1016/j.jms.2008.06.012> (2008).
131. Kassi, S., Song, K. F. & Campargue, A. High sensitivity CW-cavity ring down spectroscopy of ¹²CO₂ near 1.35 μm (I): line positions. *J. Quant. Spectrosc. Radiat. Transf.* **110**, 1801–1814, <https://doi.org/10.1016/j.jqsrt.2009.04.010> (2009).
132. Campargue, A., Song, K. F., Mouton, N., Perevalov, V. I. & Kassi, S. High sensitivity CW-Cavity Ring Down Spectroscopy of five ¹³CO₂ isotopologues of carbon dioxide in the 1.26–1.44 μm region (I): Line positions. *J. Quant. Spectrosc. Radiat. Transf.* **111**, 659–674, <https://doi.org/10.1016/j.jqsrt.2009.11.013> (2010).
133. Pastor, P. C., Galli, I., Giusfredi, G., Mazzotti, D., De Natale, P. Saturated-absorption cavity ring-down spectroscopy, in: *Frontiers in Optics 2010/Laser Science XXVI*, Vol. 104 of *FIO, OSA*, 2010, p. FTuL4. <https://doi.org/10.1364/fio.2010.ftul4>
134. Song, K. F., Kassi, S., Tashkun, S. A., Perevalov, V. I. & Campargue, A. High sensitivity CW-cavity ring down spectroscopy of ¹²CO₂ near 1.35 μm (II): New observations and line intensities modeling. *J. Quant. Spectrosc. Radiat. Transf.* **111**, 332–344, <https://doi.org/10.1016/j.jqsrt.2009.09.004> (2010).

135. Gatti, D. *et al.* Absolute frequency spectroscopy of CO₂ lines at around 2.09 μm by combined use of an Er:fiber comb and a Ho:YLF amplifier. *Opt. Lett.* **36**, 3921–3, <https://doi.org/10.1364/OL.36.003921> (2011).
136. Gatti, D. *et al.* High-precision molecular interrogation by direct referencing of a quantum-cascade-laser to a near-infrared frequency comb. *Opt. Expr.* **19**, 17520, <https://doi.org/10.1364/oe.19.017520> (2011).
137. Song, K.-F. *et al.* High sensitivity cavity ring down spectroscopy of CO₂ overtone bands near 790 nm. *J. Quant. Spectrosc. Rad. Transf.* **112**, 761–768, <https://doi.org/10.1016/j.jqsrt.2010.11.006> (2011).
138. Cappelli, F. *et al.* Subkilohertz linewidth room-temperature mid-infrared quantum cascade laser using a molecular sub-doppler reference. *Opt. Lett.* **37**, 4811, <https://doi.org/10.1364/ol.37.004811> (2012).
139. Gambetta, A. *et al.* Comb-assisted spectroscopy of CO₂ absorption profiles in the near- and mid-infrared regions. *Appl. Phys. B* **109**, 385–390, <https://doi.org/10.1007/s00340-012-4947-3> (2012).
140. Jacquemart, D. *et al.* Infrared spectroscopy of CO₂ isotopologues from 2200 to 7000 cm⁻¹: I—Characterizing experimental uncertainties of positions and intensities. *J. Quant. Spectrosc. Radiat. Transf.* **113**, 961–975, <https://doi.org/10.1016/j.jqsrt.2012.02.020> (2012).
141. Lyulin, O. M. *et al.* Infrared spectroscopy of ¹⁷O- and ¹⁸O-enriched carbon dioxide in the 1700–8300 cm⁻¹ wavenumber region. *J. Quant. Spectrosc. Radiat. Transf.* **113**, 2167–2181, <https://doi.org/10.1016/j.jqsrt.2012.06.028> (2012).
142. Galli, I. *et al.* Absolute frequency measurements of CO₂ transitions at 4.3 μm with a comb-referenced quantum cascade laser. *Mol. Phys.* **111**, 2041–2045, <https://doi.org/10.1080/00268976.2013.782436> (2013).
143. Liao, C.-C., Lien, Y.-H., Wu, K.-Y., Lin, Y.-R. & Shy, J.-T. Widely tunable difference frequency generation source for high-precision mid-infrared spectroscopy. *Opt. Expr.* **21**, 9238, <https://doi.org/10.1364/oe.21.009238> (2013).
144. Lu, Y. *et al.* Line parameters of the 782 nm band of CO₂. *Astrophys. J.* **775**, 71, <https://doi.org/10.1088/0004-637X/775/1/71> (2013).
145. Petrova, T. M. *et al.* Measurements of ¹²C¹⁶O₂ line parameters in the 8790–8860, 9340–9650 and 11,430–11,505 cm⁻¹ wavenumber regions by means of Fourier transform spectroscopy. *J. Quant. Spectrosc. Rad. Transf.* **124**, 21–27, <https://doi.org/10.1016/j.jqsrt.2013.03.017> (2013).
146. Long, D. A., Truong, G.-W., Hodges, J. T. & Miller, C. E. Absolute ¹²C¹⁶O₂ transition frequencies at the kHz-level from 1.6 to 7.8 μm. *J. Quant. Spectrosc. Rad. Transf.* **130**, 112–115, <https://doi.org/10.1016/j.jqsrt.2013.07.001> (2013).
147. Truong, G.-W. *et al.* Comb-linked, cavity ring-down spectroscopy for measurements of molecular transition frequencies at the the kHz-level. *J. Chem. Phys.* **138**, <https://doi.org/10.1063/1.4792372> (2013).
148. Borkov, Y. G., Jacquemart, D., Lyulin, O. M., Tashkun, S. A. & Perevalov, V. I. Infrared spectroscopy of ¹⁷O- and ¹⁸O-enriched carbon dioxide: Line positions and intensities in the 3200–4700 cm⁻¹ region. Global modeling of the line positions of ¹⁶O¹²C¹⁷O and ¹⁷O¹²C¹⁷O. *J. Quant. Spectrosc. Radiat. Transf.* **137**, 57–76, <https://doi.org/10.1016/j.jqsrt.2013.11.008> (2014).
149. Karlovets, E. V., Kassi, S., Tashkun, S. A., Perevalov, V. I. & Campargue, A. High sensitivity cavity ring down spectroscopy of carbon dioxide in the 1.19–1.26 μm region. *J. Quant. Spectrosc. Radiat. Transf.* **144**, 137–153, <https://doi.org/10.1016/j.jqsrt.2014.04.001> (2014).
150. Burkart, J. *et al.* Communication: Saturated CO₂ absorption near 1.6 μm for kilohertz-accuracy transition frequencies. *J. Chem. Phys.* **142**, 191103, <https://doi.org/10.1063/1.4921557> (2015).
151. Borkov, Y. G., Jacquemart, D., Lyulin, O. M., Tashkun, S. A. & Perevalov, V. I. Infrared spectroscopy of ¹⁷O- and ¹⁸O-enriched carbon dioxide: Line positions and intensities in the 4681–5337 cm⁻¹ region. *J. Quant. Spectrosc. Radiat. Transf.* **159**, 1–10, <https://doi.org/10.1016/j.jqsrt.2015.02.019> (2015).
152. Gatti, D. *et al.* Comb-locked cavity ring-down spectrometer. *J. Chem. Phys.* **142**, <https://doi.org/10.1063/1.4907939> (2015).
153. Lamouroux, J. *et al.* CO₂ line-mixing database and software update and its tests in the 2.1 μm and 4.3 μm regions. *J. Quant. Spectrosc. Radiat. Transf.* **151**, 88–96, <https://doi.org/10.1016/j.jqsrt.2014.09.017> (2015).
154. Jacquemart, D., Borkov, Y. G., Lyulin, O. M., Tashkun, S. A. & Perevalov, V. I. Fourier transform spectroscopy of CO₂ isotopologues at 1.6 μm: Line positions and intensities. *J. Quant. Spectrosc. Radiat. Transf.* **160**, 1–9, <https://doi.org/10.1016/j.jqsrt.2015.03.016> (2015).
155. Long, D. A., Wójciewicz, S., Miller, C. E. & Hodges, J. T. Frequency-agile, rapid scanning cavity ring-down spectroscopy (FARS-CRDS) measurements of the (30012) ← (00001) near-infrared carbon dioxide band. *J. Quant. Spectrosc. Rad. Transf.* **161**, 35–40, <https://doi.org/10.1016/j.jqsrt.2015.03.031> (2015).
156. Petrova, T. M. *et al.* Measurements of CO₂ line parameters in the 9250–9500 cm⁻¹ and 10,700–10,860 cm⁻¹ regions. *J. Quant. Spectrosc. Radiat. Transf.* **164**, 109–116, <https://doi.org/10.1016/j.jqsrt.2015.06.001> (2015).
157. Tan, Y. *et al.* Cavity ring-down spectroscopy of CO₂ overtone bands near 830 nm. *J. Quant. Spectrosc. Rad. Transf.* **165**, 22–27, <https://doi.org/10.1016/j.jqsrt.2015.06.010> (2015).
158. Benner, D. C. *et al.* Line parameters including temperature dependences of air- and self-broadened line shapes of ¹²C¹⁶O₂: 2.06-μm region. *J. Mol. Spectrosc.* **326**, 21–47, <https://doi.org/10.1016/j.jms.2016.02.012> (2016).
159. Devi, V. M. *et al.* Line parameters including temperature dependences of self- and air-broadened line shapes of ¹²C¹⁶O₂: 1.6-μm region. *J. Quant. Spectrosc. Radiat. Transf.* **177**, 117–144, <https://doi.org/10.1016/j.jqsrt.2015.12.020> (2016).
160. Vasilchenko, S. *et al.* The CO₂ absorption spectrum in the 2.3 μm transparency window by high sensitivity CRDS: (I) Rovibrational lines. *J. Quant. Spectrosc. Radiat. Transf.* **184**, 233–240, <https://doi.org/10.1016/j.jqsrt.2016.07.002> (2016).
161. Guan, Y.-C. *et al.* Frequency measurements and molecular constants of the ¹²C¹⁶O₂[10⁰1, 02¹]_{II} ← 00⁰0 band near 2.7 μm. *J. Mol. Spectrosc.* **334**, 26–30, <https://doi.org/10.1016/j.jms.2017.03.011> (2017).
162. Kassi, S., Karlovets, E. V., Tashkun, S. A., Perevalov, V. I. & Campargue, A. Analysis and theoretical modeling of the ¹⁸O enriched carbon dioxide spectrum by CRDS near 1.35 μm: (I) ¹⁶O¹²C¹⁸O, ¹⁶O¹²C¹⁷O, ¹²C¹⁶O₂ and ¹³C¹⁶O₂. *J. Quant. Spectrosc. Radiat. Transf.* **187**, 414–425, <https://doi.org/10.1016/j.jqsrt.2016.09.002> (2017).
163. Čermák, P. *et al.* High sensitivity CRDS of CO₂ in the 1.74 μm transparency window. A validation test for the spectroscopic databases. *J. Quant. Spectrosc. Radiat. Transf.* **207**, 95–103, <https://doi.org/10.1016/j.jqsrt.2017.12.018> (2018).
164. Karlovets, E. V. *et al.* Analysis and theoretical modeling of the ¹⁸O enriched carbon dioxide spectrum by CRDS near 1.74 μm. *J. Quant. Spectrosc. Radiat. Transf.* **217**, 73–85, <https://doi.org/10.1016/j.jqsrt.2018.05.017> (2018).
165. Gotti, R. *et al.* Comb-locked-frequency-swept synthesizer for high precision broadband spectroscopy. *Sci. Rep.* **10**, 2523, <https://doi.org/10.1038/s41598-020-59398-1> (2020).
166. Karlovets, E. V., Kassi, S. & Campargue, A. High sensitivity CRDS of CO₂ in the 1.18 μm transparency window. Validation tests of current spectroscopic databases. *J. Quant. Spectrosc. Radiat. Transf.* **247**, 106942, <https://doi.org/10.1016/j.jqsrt.2020.106942> (2020).
167. Lamperti, M. *et al.* Optical frequency metrology in the bending modes region, *Commun. Phys.* **3** <https://doi.org/10.1038/s42005-020-00441-y> (2020).
168. Reed, Z. D., Long, D. A., Fleurbaey, H. & Hodges, J. T. SI-traceable molecular transition frequency measurements at the 10⁻¹² relative uncertain level. *Optica* **7**, 1209–1220, <https://doi.org/10.1364/OPTICA.395943> (2020).
169. Wu, H. *et al.* A well-isolated vibrational state of CO₂ verified by near-infrared saturated spectroscopy with kHz accuracy. *Phys. Chem. Chem. Phys.* **22**, 2841–2848, <https://doi.org/10.1039/C9CP05121J> (2020).
170. Predoi-Cross, A. & Buldyrev, J. Characterization of line mixing effects in the 11101 ← 00001 band of carbon dioxide for pressures up to 19 atm. *J. Quant. Spectrosc. Radiat. Transf.* **272**, 107793, <https://doi.org/10.1016/j.jqsrt.2021.107793> (2021).
171. Reed, Z. D., Drouin, B. J., Long, D. A. & Hodges, J. T. Molecular transition frequencies of CO₂ near 1.6 μm with kHz-level uncertainties. *J. Quant. Spectrosc. Rad. Transf.* **271**, 107681, <https://doi.org/10.1016/j.jqsrt.2021.107681> (2021).

172. Marinina, A. A. *et al.* Absorption spectrum of carbon dioxide in the 4350–4550 cm⁻¹ region. *Atmos. Ocean. Opt.* **35**, 8–13, <https://doi.org/10.1134/s1024856022010109> (2022).
173. Tan, Y. *et al.* Cavity-enhanced saturated absorption spectroscopy of the (30012) - (00001) band of ¹²C¹⁶O₂. *J. Chem. Phys.* **156**, 044201, <https://doi.org/10.1063/5.0074713> (2022).
174. Chen, T. Y., Steinmetz, S. A., Patterson, B. D., Jasper, A. W. & Kliewer, C. J. Direct observation of coherence transfer and rotational-to-vibrational energy exchange in optically centrifuged CO₂ super-rotors. *Nat. Commun.* **14**, 3227, <https://doi.org/10.1038/s41467-023-38873-z> (2023).
175. Fleurbaey, H. *et al.* ¹²CO₂ transition frequencies with kHz-accuracy by saturation spectroscopy in the 1.99–2.09 μm region. *Phys. Chem. Chem. Phys.* **25**, 16319–16330, <https://doi.org/10.1039/D3CP01603J> (2023).
176. Lyulin, O. M., Solodov, A. M., Solodov, A. A., Petrova, T. M. & Perevalov, V. I. The absorption bands of ¹²C¹⁶O₂ near 718 nm. *J. Quant. Spectrosc. Rad. Transf.* **303**, 108595, <https://doi.org/10.1016/j.jqsrt.2023.108595> (2023).
177. Birk, M., Röske, C. & Wagner, G. The pressure dependence of the experimentally-determined line intensity and continuum absorption of pure CO₂ in the 1.6 μm region. *J. Quant. Spectrosc. Rad. Transf.* **324**, 109055, <https://doi.org/10.1016/j.jqsrt.2024.109055> (2024).
178. Jiang, S., Tan, Y., Liu, A.-W., Zhou, X.-G. & Hu, S.-M. Saturated cavity ring-down spectroscopy of ¹²C¹⁶O₂ near 1.57 μm. *Chin. J. Chem. Phys.* **37**, 13–18, <https://doi.org/10.1063/1674-0068/cjcp2305046> (2024).
179. Ritter, M. E., DeSouza, S. A., Ogden, H. M., Michael, T. J. & Mullin, A. S. Transient IR spectroscopy of optically centrifuged CO₂ (R186–R282) and collision dynamics for the *J* = 244 – 282 states. *Faraday Discuss.* **251**, 140–159, <https://doi.org/10.1039/D3FD00179B> (2024).
180. Serdyukov, V. I., Sinitsa, L. N. & Vasil'chenko, S. S. Highly sensitive Fourier transform spectroscopy with LED sources. *J. Mol. Spectrosc.* **290**, 13–17, <https://doi.org/10.1016/j.jms.2013.06.004> (2013).
181. Amat, G. & Pimbert, M. On Fermi resonance in carbon dioxide. *J. Mol. Spectrosc.* **16**, 278–290, [https://doi.org/10.1016/0022-2852\(65\)90123-2](https://doi.org/10.1016/0022-2852(65)90123-2) (1965).
182. Rothman, L. S. & Young, L. D. G. Infrared energy levels and intensities of carbon dioxide-II. *J. Quant. Spectrosc. Radiat. Transf.* **25**, 505–524, [https://doi.org/10.1016/0022-4073\(81\)90026-1](https://doi.org/10.1016/0022-4073(81)90026-1) (1981).
183. Toth, R. A., Brown, L. R., Miller, C. E., Devi, V. M. & Benner, D. C. Spectroscopic database of CO₂ line parameters: 4300 – 7000 cm⁻¹. *J. Quant. Spectrosc. Radiat. Transf.* **109**, 906–921, <https://doi.org/10.1016/j.jqsrt.2007.12.004> (2008).
184. Furtenbacher, T. 626M24 dataset of ¹²C¹⁶O₂ <https://doi.org/10.17605/OSF.IO/9PZEW> (2024).

Acknowledgements

The authors thank STFC for funding the UK–Jordan collaboration under the Newton Fund grant ST/T001429/1. JT acknowledges the support of the European Research Council (ERC) under the European Union’s Horizon 2020 research and innovation programme through Advance Grant number 883830. The work of A.G.C. and F.T. received support from NKFH (grant number K138233).

Author contributions

A.A.A.A., J.T., T.F., and A.G.C. designed the study, with important contributions from the further co-authors, mainly responsible for collecting measured data. A.A.A.A., J.T., T.F., S.N.Y. and A.G.C. checked different aspects of the datasets (transitions and energy levels). A.A.A.A., J.T., and A.G.C. wrote the original version of the manuscript. All of the authors have contributed to writing the final manuscript.

Funding

Open access funding provided by Eötvös Loránd University.

Competing interests

The authors declare no competing interests.

Additional information

Correspondence and requests for materials should be addressed to A.A.A.A., J.T. or A.G.C.

Reprints and permissions information is available at www.nature.com/reprints.

Publisher’s note Springer Nature remains neutral with regard to jurisdictional claims in published maps and institutional affiliations.



Open Access This article is licensed under a Creative Commons Attribution 4.0 International License, which permits use, sharing, adaptation, distribution and reproduction in any medium or format, as long as you give appropriate credit to the original author(s) and the source, provide a link to the Creative Commons licence, and indicate if changes were made. The images or other third party material in this article are included in the article’s Creative Commons licence, unless indicated otherwise in a credit line to the material. If material is not included in the article’s Creative Commons licence and your intended use is not permitted by statutory regulation or exceeds the permitted use, you will need to obtain permission directly from the copyright holder. To view a copy of this licence, visit <http://creativecommons.org/licenses/by/4.0/>.

© The Author(s) 2025